ERNEST ORLANDO LAWRENCE
BERKELEY NATIONAL LABORATORY

CONF-971196--

Li Ion Conductors Based on Laponite/Poly(Ethylene Oxide) Composites

DISTRIBUTION OF THIS DOCUMENT IS UNLIMITED

Marca M. Doeff and John S. Reed

Materials Sciences Division

RECEIVED
DEC 17 1997
OSTI

MASTER

November 1997

Presented at the
*Solid State Ionics
Conference 1997,*
Honolulu, HI,
November 16–21, 1997,
and to be published in
the Proceedings

19980402 096

DISCLAIMER

Li ION CONDUCTORS BASED ON
LAPONITE/POLY(ETHYLENE OXIDE) COMPOSITES

Marca M. Doeff and John S. Reed

Materials Sciences Division
Lawrence Berkeley National Laboratory
University of California
Berkeley, CA 94720, USA

Li ION CONDUCTORS BASED ON LAPONITE/POLY(ETHYLENE OXIDE) COMPOSITES

Marca M. Doeff and John S. Reed
Materials Sciences Division
Lawrence Berkeley National Laboratory
University of California
Berkeley, CA 94720

Abstract

Synthesis and characterization of single-ion conducting poly(ethylene oxide) (PEO)/Li-laponite nanocomposites are reported. The amount of PEO that can be intercalated into laponite, a synthetic hectorite with high surface area, ranges from about 0.7g/g Li-laponite when the polymer average molecular weight is 1000 or above, to about 1 g/g for oligomers of average molecular weight 500. The interlayer spacing increases from about 10 Å in the dry clay to 20 -24 Å in the nanocomposites, depending upon polymer molecular weight, and the average particle size increases proportionally, but is still in the sub-micron range. AC impedance measurements on the clear, slightly brittle, self-supporting films indicate that the nanocomposite conductivity is greatly enhanced over that of the dry clay. A maximum of about 10^{-6} S/cm at 80° C is obtained for materials containing a slight excess of polymer, and conductivities of nanocomposites containing PEO were generally higher than that of those containing oxymethylene-linked polyethylene glycols (amorphous PEOs). Suggestions for further improving conductivity and mechanical properties of these novel materials are presented.

Introduction

Improved safety over conventional, fully liquid electrolytes provides a compelling rationale for use of polymer electrolytes in rechargeable lithium batteries, but these polymers often show insufficient conductivity or poor mechanical properties. The dual ion-conducting nature of most polymer electrolytes also poses problems. A recent rigorous investigation of transport properties [1] indicates that cationic transference numbers are non-unity or even negative (Figure 1), indicating substantial transport by anionic complexes, particularly at high salt concentration. Concentration gradients caused by the mobility of both cations and anions in the electrolyte arise during cell operation, resulting in premature cell failure [2]. This is a more severe problem than in conventional liquid electrolytes because of the lower salt diffusion coefficients and the relative immobility of the polymer hosts.

Attempts to design single ion conductors based on poly-electrolytes with fixed negative charges on the polymer [3] have met with limited success; conductivities are generally too low for practical use. Still, the ease of film fabrication, ability to withstand electrode volume changes, and low temperature operation of a well-designed polymer-based system provide distinct advantages over many ceramic single-ion conductors. Further research into polymeric or composite single-ion conductors is, therefore, well-justified.

Recent reports of single-ion conducting polymer- smectite intercalation compounds [4, 5, 6] indicate that conductivities are greatly enhanced over that of the dry, native clays. Preparation of these materials is much simpler, in practice, than that of the synthetic polymer single-ion conductors mentioned above and films form readily, are self-supporting, and generally have excellent mechanical properties. Only cations are mobile in these materials, sometimes termed "nanocomposites". In spite of these promising characteristics, some obstacles to their practical use remain. Preferential orientation in films so that the non-conducting planes are perpendicular to the current path, tends to occur. Naturally occurring clays are also difficult to purify and characterize. In this study a synthetic hectorite clay, Laponite RD, was used to overcome these difficulties. This layered hydrous magnesium silicate has a high degree of structural regularity and low levels of impurities. Sodium ions between the negatively charged silicate layers are readily exchanged for other ions (exchange capacity= 0.8 meq/g) (7). Laponite has an extremely high surface area (370 M^2/g) and very small particle size. This suggests that preferential orientation is less likely to occur in the synthesis of the electrolyte films. Herein, we report on the synthesis and characterization of some laponite-containing nanocomposites.

Experimental

Laponite RD was a gift from Southern Clay Products (Gonzales, Texas). Poly(ethylene oxide) (PEO) with average molecular weight 100,000, poly(ethylene glycol) dimethyl ether (PEGDME)-500 and -1000 and lithium trifluoromethaneulfonate (LiCF$_3$SO$_3$) were used as received from Aldrich Chemical Company. Lithium (bis)trifluoromethanesulfonate imide (LiTFSI) was used as received from 3M Company. Oxymethylene-linked poly(ethylene glycol)-400 and -200/400 (amorphous PEOs) were synthesized by Dr. Christian Nicholas of Manchester University, and stored in an inert atmosphere prior to use. Methyl-capped oxymethylene-linked poly(ethylene glycol)-400 was a gift from Dr. John Kerr of Lawrence Berkeley National Laboratory and was treated similarly. The amorphous PEOs all had M_n of 100,000 or more, as determined by gel permeation chromatography.

Colloidal suspensions containing 1g laponite/100 mL de-ionized water were stirred for one-half hour prior to addition of salt. LiCl was then added to the suspensions to make 1M solutions. The laponite was stirred in the 1 M LiCl solution for at least 48 hours to ensure complete ionic exchange. The suspensions were then dialyzed until the salt was completely removed. This was judged to occur when the suspensions appeared completely clear (salt-containing solutions are slightly cloudy) and no visible

precipitate was detected when 1M AgNO₃ was added to an aliquot of the suspension. The desired amount of polymer or oligomer was then added, and the mixture stirred for an additional 24 hours. For some samples, LiTFSI or LiCF₃SO₃ was added at the same time as polymer.

Films were prepared by puddle-casting solutions onto Teflon-coated glass plates or onto glass substrates and air-drying. Unless otherwise stated, further drying was carried out at 120° C under an inert atmosphere for at least 48 hours. Films were clear to translucent, and those with low polymer content (<0.3g/g Li-laponite) or those that contained the low molecular weight oligomers were brittle. Those containing more than 0.3 g polymer/g Li-laponite were less brittle, but still had good mechanical properties.

XRD patterns were obtained on as-received laponite RD, Li-exchanged laponite, and Li-exchanged laponite/polymer films cast onto glass windows, using a Siemens D500 diffractometer and Cu Kα radiation. Thermo-gravimetric analysis under nitrogen, on air-dried films, and differential scanning calorimetry under helium or nitrogen, on fully dried films, were carried out with Perkin-Elmer DSC-7 and TGA-7 instruments, at scan rates of 10° C/min. AC impedance measurements as a function of temperature were obtained on films in sealed cells with stainless steel electrodes, using a Solartron SI 1286 electrochemical interface and 1254 four-channel frequency response analyzer.

Results and Discussion

Figure 2 shows the XRD patterns of several PEO (MW=100,000)-containing Li-laponite nanocomposites, as well as that of Li-laponite itself. Relatively little structural information can be obtained from these patterns, because the peaks, although intense, are extremely broad. The 001 reflection, at low angles, is the strongest. The higher angle peaks cannot be assigned definitively at this time, but are not higher order 00ℓ reflections, judging from their positions. This indicates that there is little preferential orientation in the samples [8].

The peak width at half-height diminishes from about 4° to 2° as polymer content increases. Particles grow from about 26 Å to 57 Å in the c-direction, as determined by the Scherrer equation [9]. The number of elementary layers in the particles remain roughly constant (approximately 3 to 5), and the growth can be attributed mainly to the increased gallery height when polymer is inserted between the silicate sheets. The very small particle size and low number of elementary layers in the particles favor random orientation in films, unlike what is typically found in clay samples. Conductivity in all of the clays tends to be highly anisotropic, and preferential orientation, which tends to occur so that the non-conducting silicate sheets are parallel to the substrate increases the sample resistance by about two orders of magnitude [5, 6, 10].

Pure, dry laponite theoretically has a d(001)-spacing of about 10 Å, but films exposed to the atmosphere typically contain a mono-layer of water, which increases this to about 13.5 Å [7]. The d(001) spacing of laponite samples progressively increases with polymer content until a maximum is reached (Figure 3), which is dependent upon the molecular weight of the intercalant. For PEO (MW=100,000) and the high molecular weight amorphous-PEO containing samples, the limit is about 19-21 Å and is reached at about 0.7 g polymer/g Li-laponite. A slightly larger spacing is observed for PEGDME-1000 at a similar ratio, but for PEGDME-500, both the maximum d-spacing of about 24 Å and the limiting polymer amount of about 1.2 g/g have increased substantially. In some of the XRD patterns of samples containing more than 0.7 g PEO or PEGDME-1000, sharp peaks attributable to free, crystalline polymer or oligomer are evident.

No melting transitions are observed in the DSC experiment for materials containing less than 0.7g PEO (MW=100,000)/g laponite, indicating that all of the polymer is intercalated between the layers. A very small melting transition at 62° C was seen for the 0.7g/g sample, however, indicating that about 1% of the polymer is located outside the silicate sheets. Similar results were obtained for samples containing

amorphous PEOs. This, as well as the XRD results, indicates that the maximum amount of PEO or amorphous PEO that can be intercalated into laponite is slightly less than 0.7g/g (this corresponds to 41 w/o or 59 v/o polymer for PEO, or about 17 ethylene oxide units per Li^+). Samples containing more than this are two-phase mixtures of intercalation compounds and discrete polymers, or true composites. A similar analysis for films containing PEGDME-1000 indicate that slightly more than 0.7 g/g can be intercalated, and for PEGDME-500, a maximum of about 1.1 g (52.4 w/o, 69.7 v/o, or about 27 ethylene oxide units per Li^+).

TGA traces of laponite and polymer-laponite nanocomposites are shown in Figure 4. PEO and amorphous PEOs generally begin to decompose at about 300-350° and are completely burned away at 400° C, under the conditions of this study (10° C/min, under N_2). Weight loss below this temperature can be attributed to water evaporation. An air-dried laponite film contains about 16% water, most of which is lost below 100° C, or within the first few minutes of heating. It is apparent that the polymer-containing films, which were not subjected to heat or vacuum prior to TGA analysis, contain markedly less water than this. This indicates that the water located between the silicates sheet is readily replaced by polymer in the nanocomposites and composites, although, for materials with low polymer contents, the substitution is probably only partial. Like laponite, the nanocomposites are easily dried under vacuum or during heating, but they rapidly rehydrate upon exposure to the atmosphere. Polymer compositions calculated from the weight loss above 300° C in the TGA traces were identical to the expected values, within experimental error.

Self-supporting films of most nanocomposites and composites can be readily fabricated and have excellent mechanical properties. Those with low polymer content (< 0.3g/g) or those containing PEGDME-500 and -1000 are, however, too brittle to use in the conductivity cells used for this study, so no data is available at this time on these materials.

Complex impedance plots from data obtained on laponite nanocomposites and composites in cells with blocking electrodes consisted of depressed capacitative arcs and/or spurs at lower frequencies, which deviated markedly from the expected 90°. This non-ideal behavior is attributable to the multi-granular nature of the samples [11]. In this study, it was not possible to separate the contributions from bulk and grain boundary resistances; the reported conductivities are derived from the low frequency touchdown point of the capacitative arcs (or x-intercept of the spurs) in the Nyquist plots, without further analysis.

Arrhenius plots for representative nanocomposites, composites and salt-containing composites containing PEO (MW=100,000) or amorphous PEOs are presented in Figures 5, 6 and 7, respectively. The conductivity is dramatically increased when polymer is intercalated between the silicate layers of the clay (it is not measurable in this temperature range for absolutely dry laponite films, but is estimated to be about 10^{-19} S/cm at 25° C [5]). Single-ion conductivities as high as 10^{-6} S/cm at 80° C are found for two-phase mixtures with no added salt or plasticizer. The increase in conductivity over that of the dry clay is due both to the increased interlayer spacing and to shielding of the cations from the negatively charged silicate sheets by the intercalated polymer [4, 5, 6, 10]. Other contributing factors may be decreased grain boundary resistance and space-charge effects, when small amounts of discrete polymer are present (see, e.g., data in Figures 5 and 6 for samples containing 0.7-1.2 g polymer/g Li-laponite). When large excesses are present, the samples are extremely resistive, as expected, particularly below the polymer melting point.

Conductivities for salt-containing mixtures are much higher than those with no added salt (Figure 7), and are similar to those for simple binary salt-PEO systems without additives. These films have much better dimensional stability than those without laponite, however. The addition of a single-conducting phase to the polymer electrolyte may allow less salt to be used, reducing both the cost and the tendency towards severe concentration polarization during cell operation. Similarly, laponite may be used as a

structural element in gels containing mixtures of salt, solvents or oligomers and polymers, to confer dimensional stability.

A characteristic break in the data is seen near the polymer melting point for samples containing excess PEO of molecular weight 100,000 (Figure 6), and a changeover from Arrhenius to VTF behavior [12] occurs, indicating that segmental motion of the polymer dominates the conductivity behavior in the higher temperature region [13]. (This also serves to confirm that these systems are two-phase). No break is seen for materials containing the amorphous PEOs or for the nanocomposites which do not contain polymer as discrete phases (Figure 5). It is interesting to note that VTF behavior is also observed for many of these nanocomposites, particularly those with polymer contents near the maximum uptake limit. This suggests a free volume mechanism dominates the conductivity behavior (i.e., rather than ion-hopping from site to site, polymer segmental motion between the silicate sheets propels the ions, as in most polymer electrolytes). Even so, conductivities in the nanocomposites are much lower than those of most PEO-salt complexes. In part, this is due to the fact that nanocomposites are cationic conductors whereas both anions and cations conduct in polymer electrolytes, with anion mobility typically much greater [1]. Intercalated polymers are also essentially restricted to two dimensions between the silicate sheets, reducing their free volume considerably compared to the free polymer. VTF fits to the data in Figure 5 yield relatively high T_0 values, ranging from about 215-260 K, reflecting this reduced mobility (T_0 is typically about 30-50° C below the glass transition temperature). These results strongly suggest that conductivity can be further improved by increasing the inter-layer spacing, and/or incorporating oligomers or polar solvents. Cation motion would then be coupled to translational motion of the solvent between the layers, enhancing conductivity further. Unfortunately, our initial attempts at making such nanocomposites resulted in brittle films of little potential utility in practical devices. A possible solution to this problem is to form mixed nanocomposites containing both polymers and oligomers or solvents; these materials would have both good mechanical properties and high conductivities.

Somewhat surprisingly, nanocomposites containing amorphous PEOs generally had lower conductivities than those with PEO. This suggests that the configuration of the PEO is substantially changed by intercalation into the laponite, in such a way that ion transport is more favorable than in the intercalated amorphous PEO. The absence of thermal transitions for true nanocomposites also suggests that intercalated PEO does not have the helical conformation found in the free, crystalline polymer.

Conclusions

Difficulties in clay purification and preferential orientation leading to reduced conductivity in nanocomposites can be overcome by using synthetic hectorites with high surface area such as Laponite RD. The potential for overcoming salt concentration gradient effects in operating cells by utilizing single ion conductors, and the ease of synthesis and fabrication of nanocomposite thin films make these promising materials for applications, such as lithium rechargeable batteries, in which the use of solid electrolytes conveys a safety advantage. While conductivities of the materials reported herein are still too low for practical use, the temperature behavior strongly suggests that cation mobility is correlated with segmental mobility of the polymer intercalant. By increasing inter-layer spacings and/or intercalating mobile polar oligomers or solvents into the clays, cation motion may be coupled to the translational motion of the intercalant, greatly enhancing conductivity. Addition of small amounts of polymer to these nanocomposites would reduce the tendency to film brittleness, resulting in materials with good structural stability.
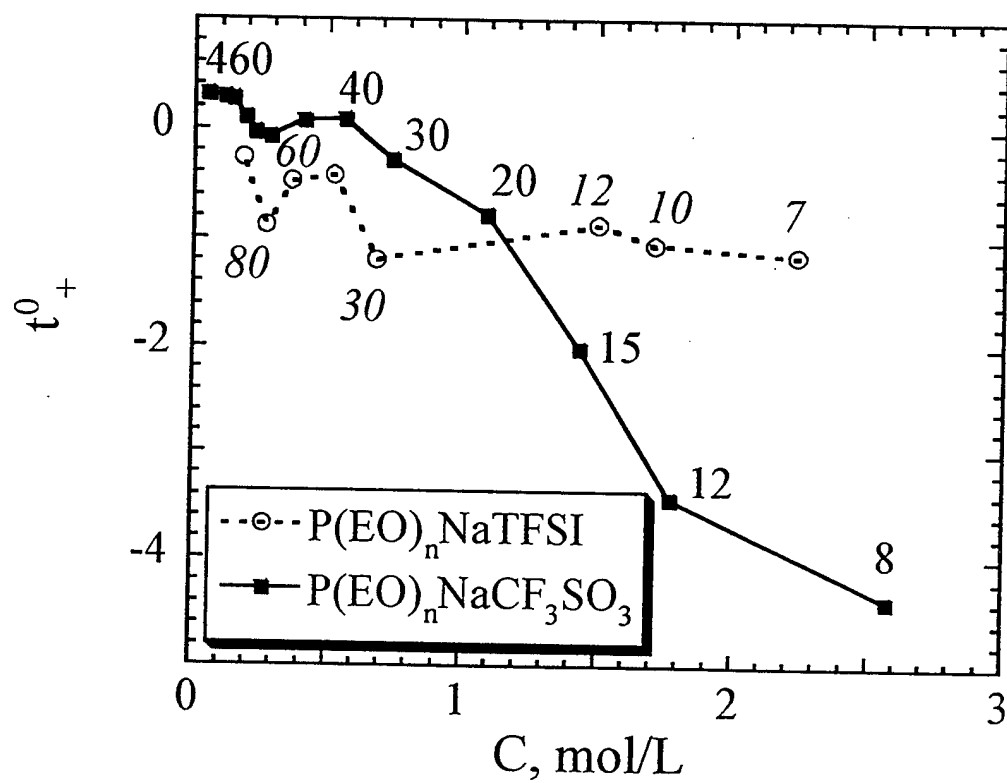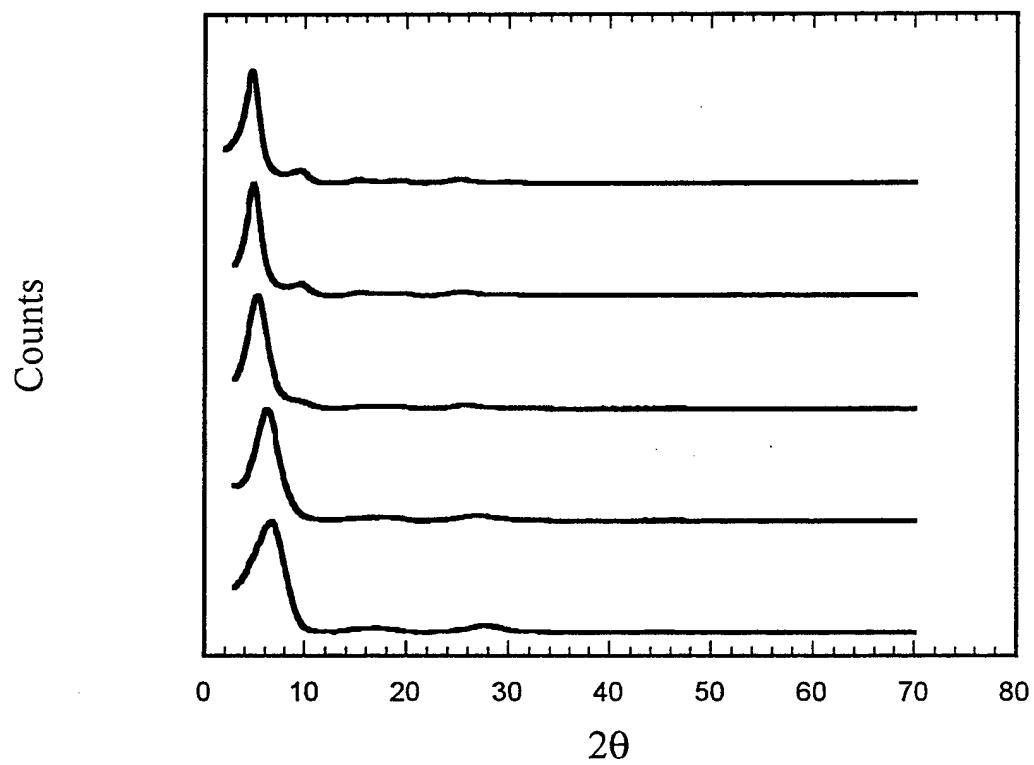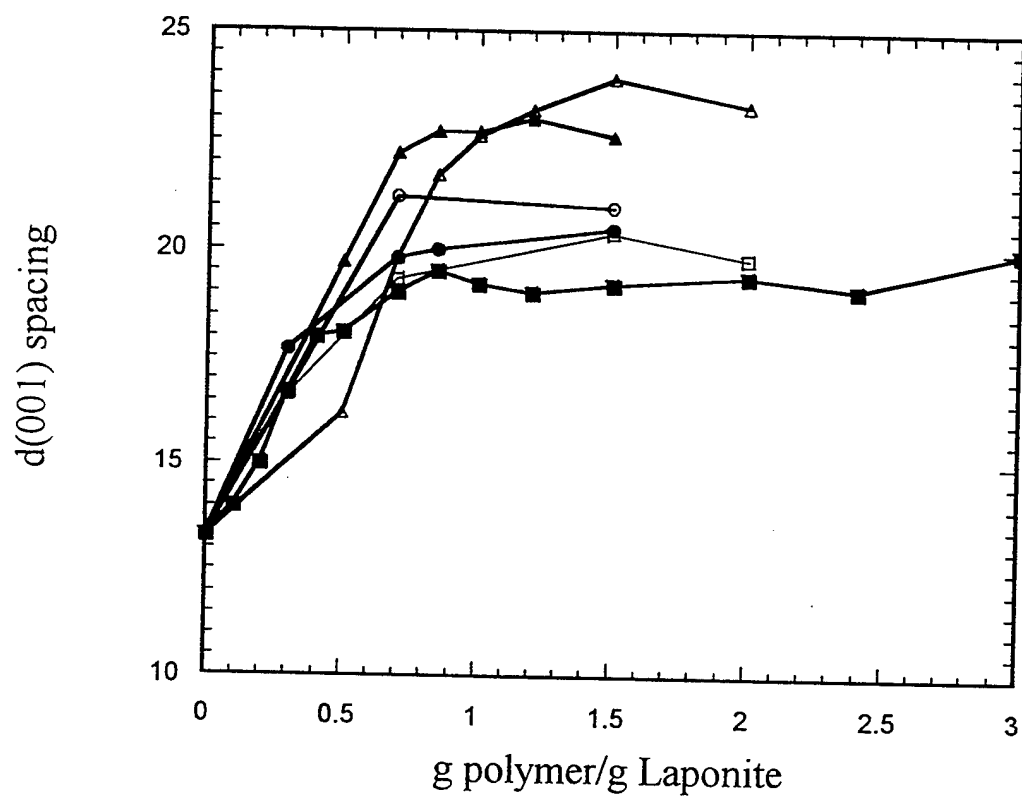
References

1) A. Ferry, M. M. Doeff and L. C. De Jonghe, *Electrochim. Acta* in press.

2) M. M. Doeff, A. Ferry, Y. Ma, L. Ding and L.C. De Jonghe, *J. Electrochem. Soc.*, **144**, L20 (1997).

3) L. C. Hardy and D. F. Shriver, *J. Am. Chem. Soc.*, **107**, 3823 (1985).

4) J. Wu and M. M. Lerner, *Chem. Mater.*, **5**, 835 (1993).

5) P. Aranda and E. Ruiz-Hutsky, *Chem. Mater.*, **4**, 1395 (1992).

6) P. Aranda and E. Ruiz-Hutsky, *Acta Polymer.*, **45**, 59 (1994).

7) P. Labbe and G. Reverdy, *Langmuir*, **4**, 419 (1988).

8) R. C. Reynolds, Jr. in *Modern Powder Diffraction*, (D. L. Post and J.E. Bish, eds.), The Mineralogical Society of America, Washington DC, 1989, p. 168.

9) R. Jenkins in *Modern Powder Diffraction*, (D. L. Post and J.E. Bish, eds.), The Mineralogical Society of America, Washington DC, 1989, p. 66.

10) E. Ruiz-Hutsky and P. Aranda, *Adv. Mater.*, **2**, 545 (1990).

11) I. D. Raistrick, C. Ho, and R. A. Huggins, *J. Electrochem. Soc.*, **123**, 1469 (1976).

12) C. A. Angell, *J. Phys. Chem.*, **68**, 1917 (1964).

13) M. A. Ratner in *Polymer Electrolyte Reviews, Vol. 1*, (J. R. MacCallum and C. A. Vincent, eds.) Elsevier Applied Science, London 1987, Chapter7.
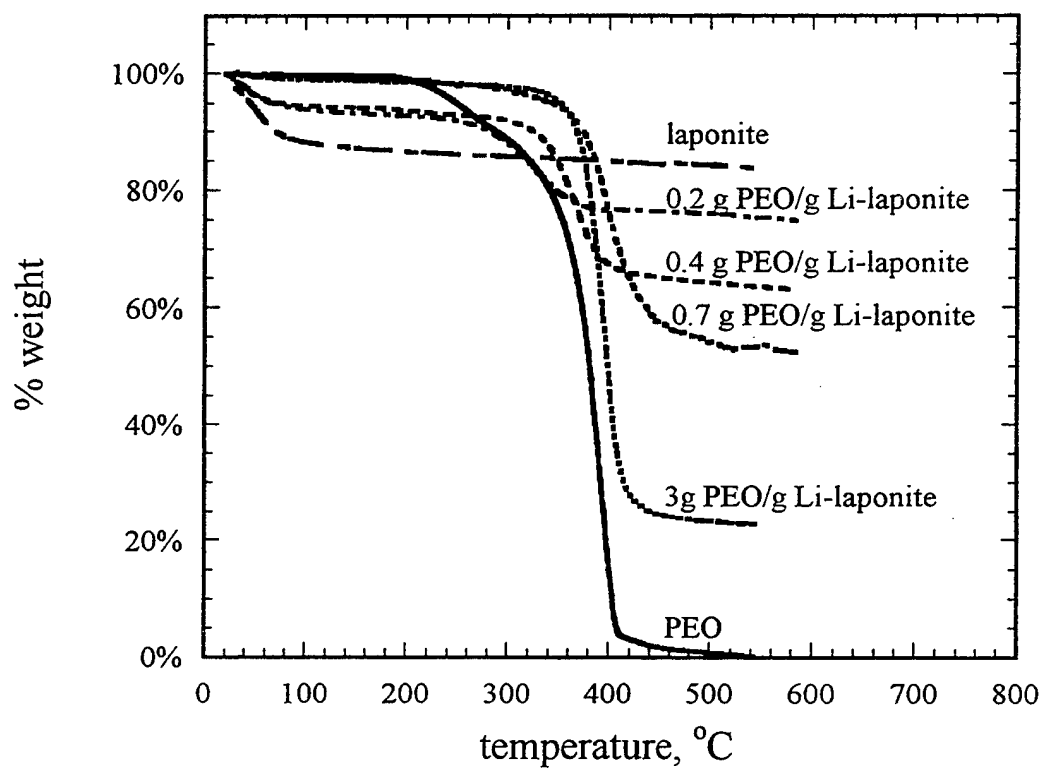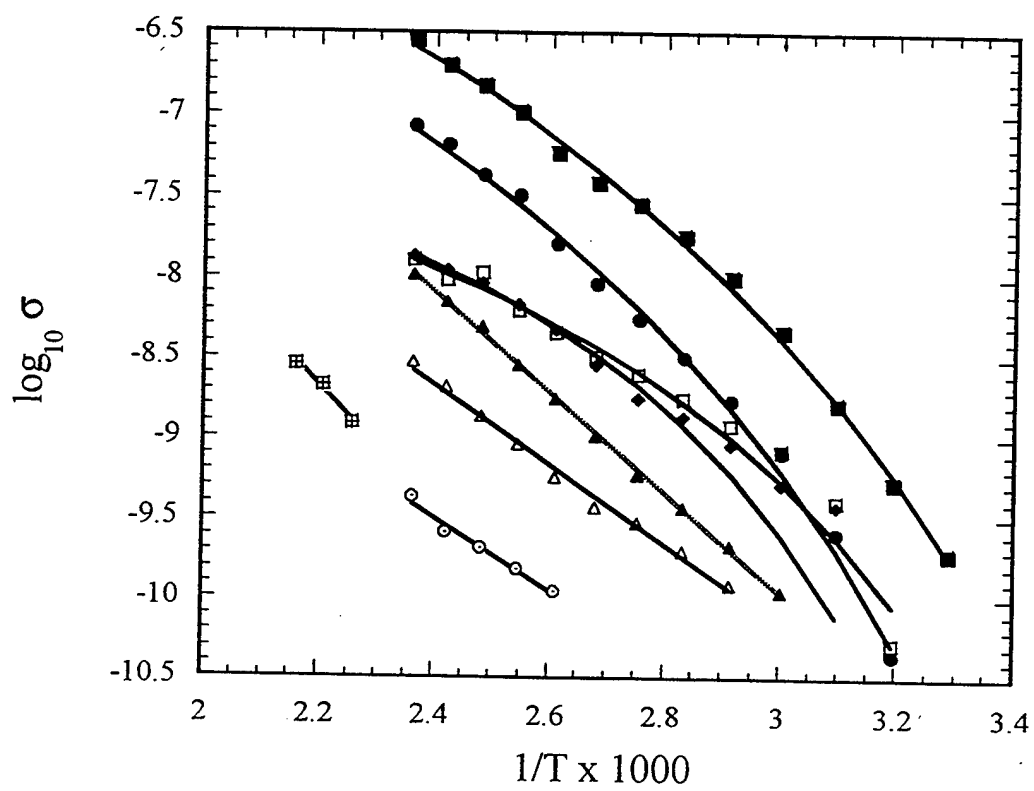
Figure Captions

1) Cationic transference numbers for polymer electrolytes at 85° C as a function of salt concentration. The number of ethylene oxide units per Na^+ are shown above each data point.

2) XRD patterns of laponite and laponite-PEO (MW=100,000) films. From bottom to top: Li-laponite, 0.1 g PEO/g Li-laponite, 0.3 g PEO/g Li-laponite, 0.5 g PEO/g Li-laponite, 0.7 g PEO/g Li-laponite.

3) d(001) spacings for laponite-polymer samples. PEO, MW=100,000 (■), oxymethylene-linked PEG-400 (□), methyl capped oxymethylene-linked PEG-400 (●), oxymethylene-linked PEG-200/400 (O), PEGDME-1000 (▲), PEGDME-500 (Δ).

4) TGA (10° C/min, under N_2) traces for PEO, laponite, and several laponite-PEO films. From bottom to top (on the right-hand side), PEO, 3g PEO/g Li-laponite, 0.7g PEO/g Li-laponite, 0.4 g PEO/g Li-laponite, 0.2 g PEO/g Li-laponite, and laponite.

5) Arrhenius plots for Li-laponite nanocomposites. 0.3g PEO/g Li-laponite(⊞), 0.5g PEO/g Li-laponite (□), 0.7g PEO/g Li-laponite (■), 0.3g oxymethylene-linked PEG400/g Li-laponite (⊙), 0.7g oxymethylene-linked PEG400/g Li-laponite (●). 0.5g linked PEG200-400/g Li-laponite (Δ), 0.7g linked PEG200-400 /g Li-laponite (▲), 0.7 g methyl-capped oxymethylene linked PEG400/g (◆).

6) Arrhenius plots for Li-laponite-containing composites. 0.85 g PEO/g Li-laponite (■), 1g PEO/g Li-laponite (□), 1.2 g PEO/g Li-laponite (⊞), 0.85 g oxymethylene-linked PEG 200-400 (▲), 0.85 g methyl-capped oxymethylene-linked PEG 400 (◆), 1.2 g methyl-capped oxymethylene-linked PEG 400 (◊).

7) Arrhenius plots for films containing 3g PEO/g Li-laponite and salts with the following stoichiometries: $P(EO)_8LiTFSI$ (⊞), $PEO_{12}LiTFSI$ (□), $PEO_{20}LiTFSI$ (■), $PEO_{20}LiCF_3SO_3$ (●).

Counts

2θ

d(001) spacing

g polymer/g Laponite

Doeff and Reed, Figure 4
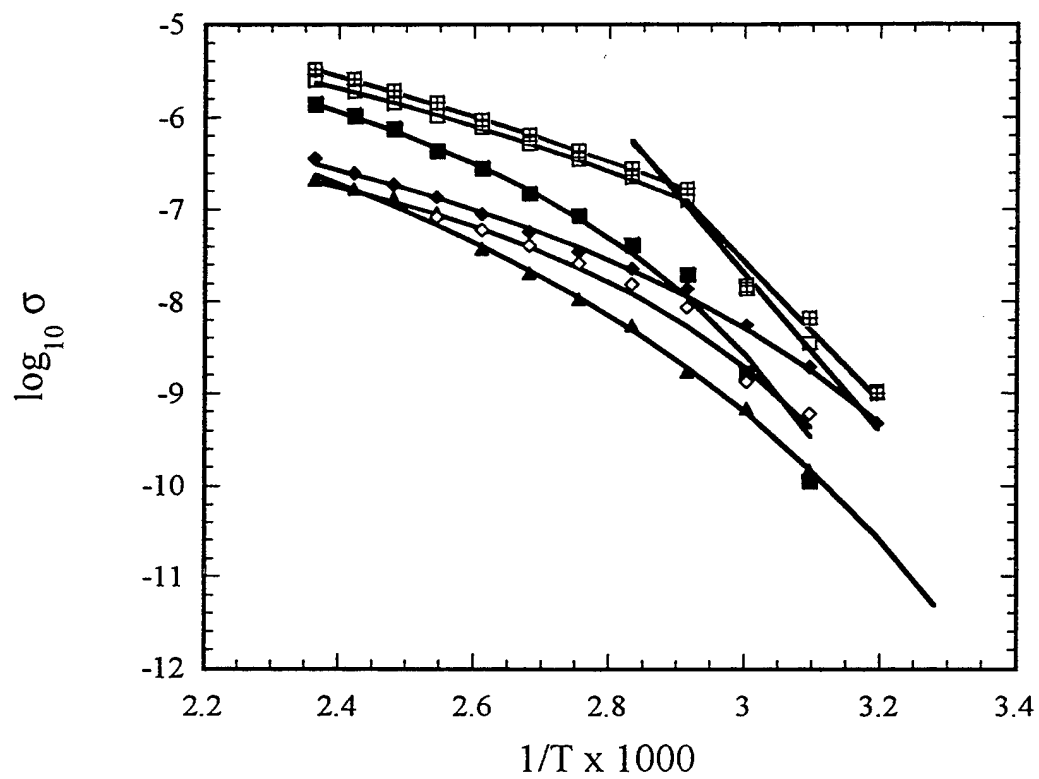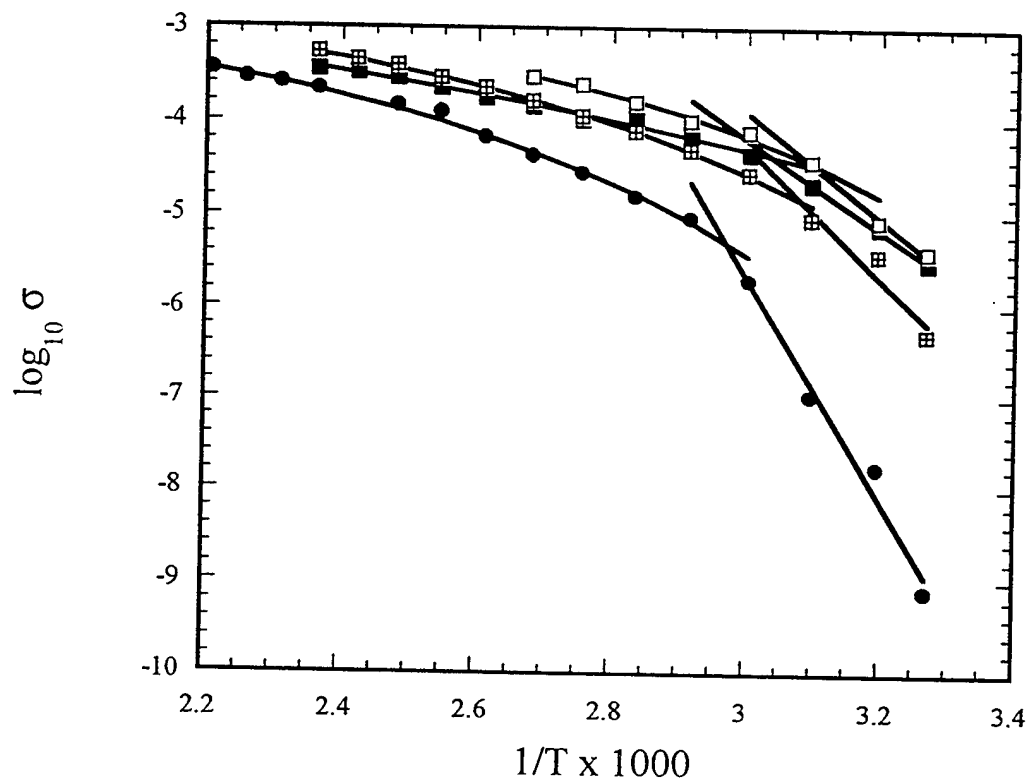
11

$\log_{10} \sigma$

1/T x 1000

Report Number (14) LBNL--41050
CONF-971196--

Publ. Date (11) 1997/1
Sponsor Code (18) DOE/EE , XF
UC Category (19) UC-1500, DOE/ER

DOE